Ab Initio Calculations of ^{31}P NMR Chemical Shielding Anisotropy Tensors in Phosphates: Variations Due to Ring Formation[†]

Todd M. Alam

Department of Organic Materials, Sandia National Laboratories, MS-0888, Albuquerque, NM 87185-0888, USA

Tel.: (505) 844-1225, Fax: (505) 844-9624, E-mail: tmalam@sandia.gov

URL: http://www.sandia.gov

Abstract: Ring formation in phosphate systems is expected to influence both the magnitude and orientation of the phosphorus (^{31}P) nuclear magnetic resonance (NMR) chemical shielding anisotropy (CSA) tensor. *Ab initio* calculations of the ^{31}P CSA tensor in both cyclic and acyclic phosphate clusters were performed as a function of the number of phosphate tetrahedral in the system. The calculation of the ^{31}P CSA tensors employed the GAUSSIAN 98 implementation of the gauge-including atomic orbital (GIAO) method at the Hartree-Fock (HF) level. It is shown that both the ^{31}P CSA tensor anisotropy, and the isotropic chemical shielding can be used for the identification of cyclic phosphates. The differences between the ^{31}P CSA tensor in acyclic and cyclic phosphate systems become less pronounced with increasing number of phosphate groups within the ring. The orientation of the principal components for the ^{31}P CSA tensor shows some variation due to cyclization, most notably with the smaller, highly strained ring systems.

Keywords: NMR, *ab initio*, ^{31}P, GIAO, Chemical shielding anisotropy, CSA, Tensor, Hartree-Fock, Phosphates, Rings, Cyclization.

Introduction

The calculation of nuclear magnetic resonance (NMR) parameters using *ab initio* techniques has become a major and powerful tool in the investigation of molecular structure. The ability to quickly evaluate and correlate the magnitude and orientation of the chemical shielding anisotropy (CSA) tensor with variations in bond angles, bond length, local coordination number and nearest-neighbor interactions has seen a number of recent applications in the investigation of molecular structure [1]. Determination of the structure and medium range order (MRO) in amorphous phosphate systems continues to be of interest in our laboratory. In particular, we are interested in utilizing *ab initio* computational techniques to look at how variations in the molecular structure impact the resulting ^{31}P NMR observables. For phosphate systems there have been a limited number of semi-empirical and *ab initio* calculation of NMR parameters reported [2-7]. One of the structural variations that has received little attention is the effect of ring formation on the magnitude and orientation of the ^{31}P CSA tensor within phosphate systems.

The formation of rings in complex systems is often forwarded to explain anomalous or unique physical properties. For example, recent molecular dynamic (MD) simulations have suggested that the MRO, including the formation of strained rings, in lithium ultraphosphate glasses may play an important role in the observed thermodynamic behavior [8]. The experimental verification of significant ring formation in these alkali phosphate glasses has yet to be realized. The aim of this paper is to determine if there are specific ^{31}P CSA tensor parameters that can be used as markers for the existence of phosphate rings in complex amorphous systems. To address the impact of ring formation on the resulting ^{31}P NMR CSA tensor, a series of *ab initio* calculations for phosphate clusters of different sizes, ranging from two to six phosphate tetrahedra are presented.

Theoretical Method

The ^{31}P CSA tensors and the energy minimized structures for both the acyclic and cyclic phosphate clusters were calculated using the parallel version of the GAUSSIAN 98 software package [9] on an eight-node DEC ALPHA computer. The gauge-including atomic orbital (GIAO) method [10] at the Hartree-Fock (HF) level of theory were employed. Investigations of basis set dependence of ^{31}P CSA tensor have been reported [11], including a detailed comparison between HF and DFT methods in phosphates [4], and will not be detailed here. The ^{31}P NMR shielding results presented were obtained using HF methods and the 6-311++G(2d,2p) basis set. All geometry optimizations employed HF methods using a 6-31+G(d) basis set. Additional details about the optimized clusters, including structural details and effective ring strain energies will be presented elsewhere (T. M. Alam, in preparation).

Typically it is only necessary to report the three principal components (or eigenvalues) of the ^{31}P CSA tensor (σ_{11}, σ_{22}, σ_{33}) when discussing the magnitude of the shielding tensor. When the ^{31}P CSA

tensor is described within the principal axis system (PAS), the diagonal representation of the tensor is obtained. Additional information about the PAS, and how it is related to the molecular axis system, is given in the later results section on ^{31}P CSA tensor orientation.

The ^{31}P CSA tensor can also be described by three additional parameters; a) the isotropic value (or trace), σ_{iso}, of the shielding tensor which is defined as

$$\sigma_{iso} = \frac{1}{3}\left(\sigma_{11} + \sigma_{22} + \sigma_{33}\right),$$ (1)

b) the anisotropy ($\Delta\sigma$) of the tensor, given by

$$\Delta\sigma = \sigma_{33} - \frac{1}{2}\left(\sigma_{22} + \sigma_{11}\right),$$ (2)

and, c) the shielding tensor asymmetry parameter (η) given by

$$\eta = \frac{\left(\sigma_{22} - \sigma_{11}\right)}{\left(\sigma_{33} - \sigma_{iso}\right)}.$$ (3)

The assignment or ordering of the principal components in the ^{31}P CSA tensor depends on the convention used, but for this manuscript the principal components are defined using

$$\left|\sigma_{33} - \sigma_{iso}\right| \geq \left|\sigma_{11} - \sigma_{iso}\right| \geq \left|\sigma_{22} - \sigma_{iso}\right|.$$ (4)

Results: Calculation of Chemical Shielding Anisotropy Tensors

Effect of Cyclization on the Magnitude and Anisotropy of the CSA Tensor

The changes in the ^{31}P CSA tensors due to ring formation for a series of phosphate clusters are reported. We were particularly interested in highly condensed and cross-linked phosphate systems, such as might be observed in phosphate glasses. While there have been recent advances in *ab initio* techniques for calculations of NMR parameters in large periodic systems [12], the *ab initio* method utilized in the present study requires the selection of isolated clusters for the actual calculations. To obtain these isolated clusters the explicit bonding or cross-linking to adjacent phosphate species is removed, with terminal P-OH groups taking the role of P-O-P linkages. In this manner it is possible to obtain clusters of manageable size for the geometry optimization and chemical shielding calculations.
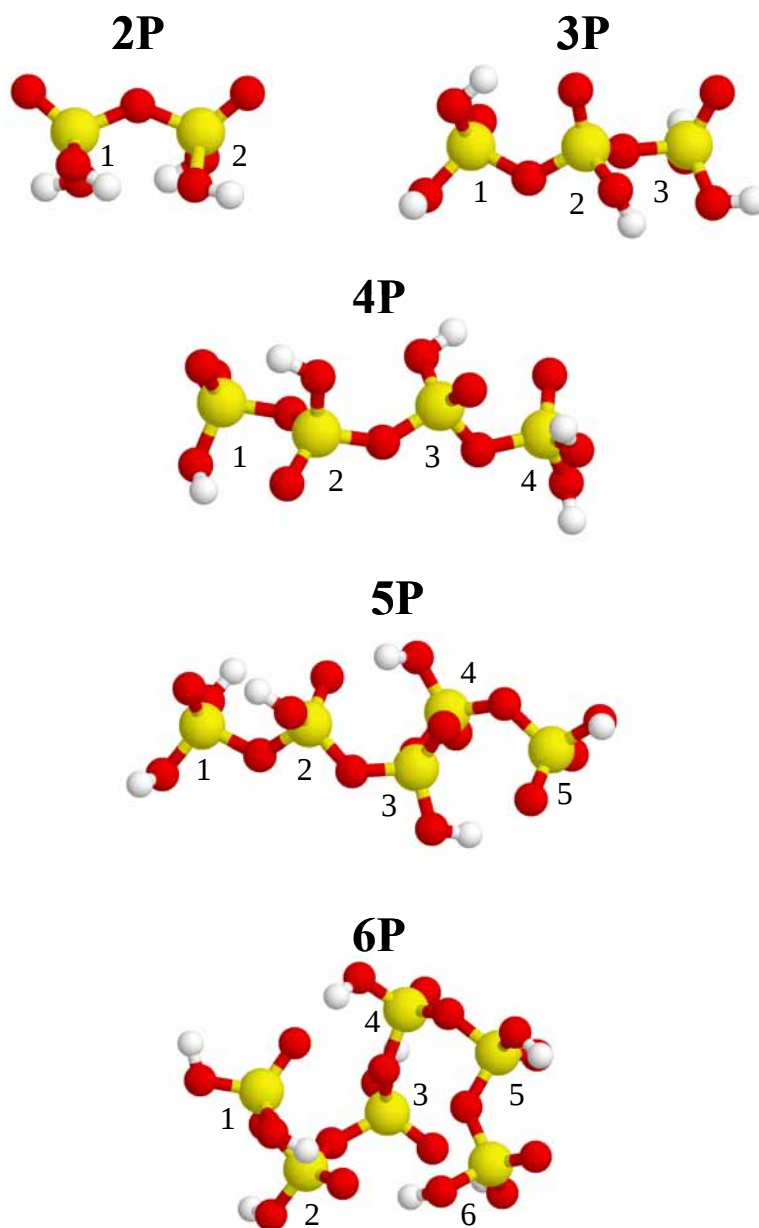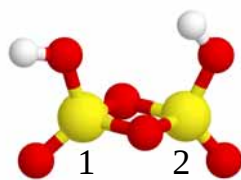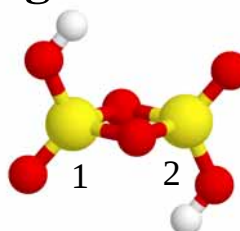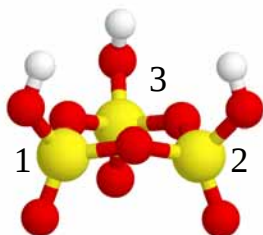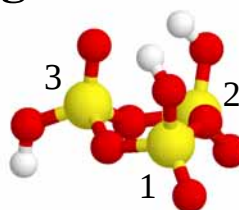
Figure 1. Different optimized conformations for 2-P, 3-P, 4-P, 5-P and 6-P-membered acyclic phosphate clusters. Phosphorus is depicted as yellow, oxygen is red, and hydrogen is white. Each phosphorus nuclei has a number ID for identification with ^{31}P CSA tensor values listed in Table 1.
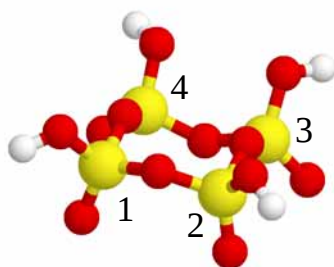
2-P Rings

(*cis*, + +)   (*trans*, + −)
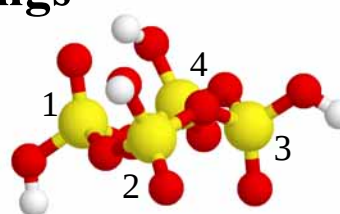
3-P Rings

(*cone*, + + +)   (*partial cone*, + + −)
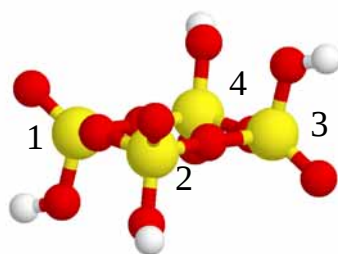
4-P Rings

(+ + + +)   (+ + + −)

(+ + − −)   (+ − + −)
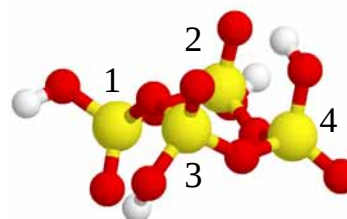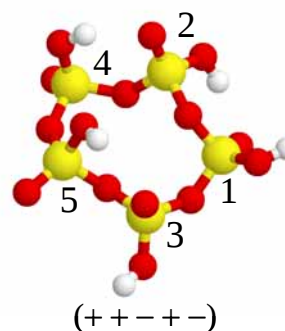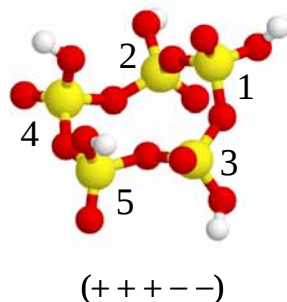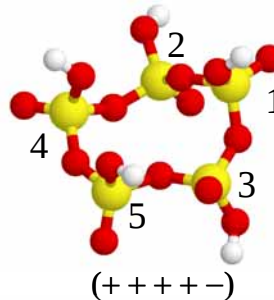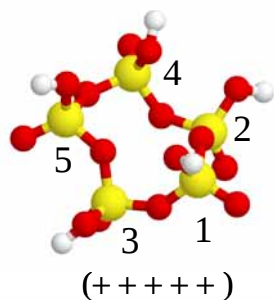
Figure 2. Different conformations for 2-P, 3-P, and 4-P-membered cyclic phosphate clusters. Phosphorus is depicted as yellow, oxygen is red, and hydrogen is white. The +/ − nomenclature refers to the relative orientation of the terminal P=O bonds (see text for details). Each phosphorus nuclei has a number ID for identification with ^{31}P CSA tensor values in Table 2.

5-P Rings

(+ + + + +)

(+ + + + −)

(+ + + − −)

(+ + − + −)

6-P Rings

(+ + + + + +)

(+ + + + + −)

(+ + + − − −)

(+ + + + − −)

(+ + + − + −)

(+ − + − + −)
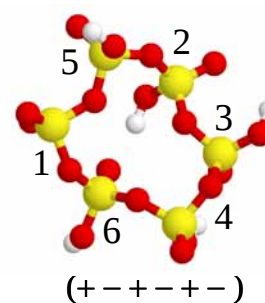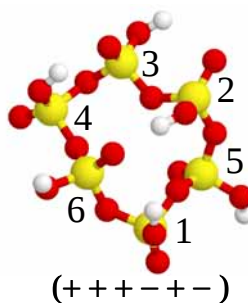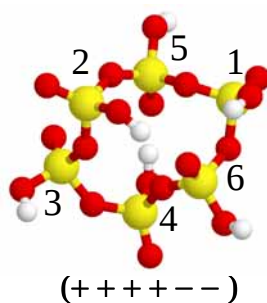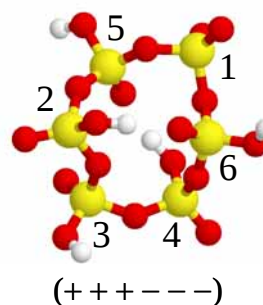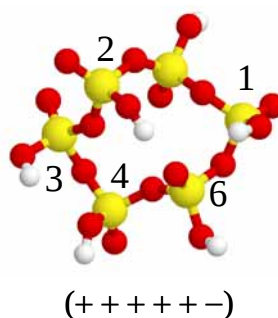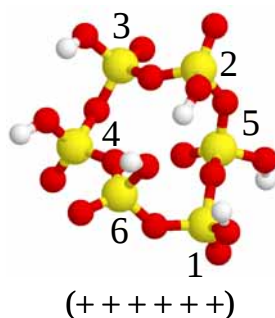
Figure 3. Different conformations for 5-P and 6-P-membered cyclic clusters investigated. Phosphorus is depicted as yellow, oxygen is red, and hydrogen is white. The +/ − nomenclature refers to the relative orientation of the terminal P=O bonds (see text for details). Each phosphorus nuclei has a number ID for identification with ^{31}P CSA tensor values in Tables 3 and 4.

The results presented here were aimed at determining the effects of cyclization on the ^{31}P chemical shielding in Q^3 type phosphate tetrahedral. The Q^n nomenclature designates the number of bridging P-O-P bonds (i.e. n) present on each phosphate tetrahedral. The phosphate clusters investigated therefore all contain one terminal P=O oxygen, one or two P-OH groups, and one or two P-O-P bonds. Recall that in these truncated clusters the P-OH bonds have been included to represent truncated P-O-P type bonding. It has been shown that the use of the OH substitution is more realistic than a simple H substitution during cluster truncation [13]. Due to the presence of a P-OH bond in place of a P-O-P bond, the resulting absolute values of the ^{31}P chemical shielding tensors will not match exactly with experimental values for Q^3 phosphate species, but the variations and trends observed in the ^{31}P CSA tensor as a result of cyclization can be used to predict and identify similar changes that would occur in Q^3 phosphate species. Minimized conformations for both cyclic and acyclic phosphate clusters containing between two and six phosphate tetrahedral were calculated, and are shown in Figures 1-3. These mimized conformations represent the lowest energy conformation obtained from several sequential optimization runs. For the acyclic clusters the starting structure prior to optimization was the linear extended all *trans* conformation. Note that the resulting minimized conformations observed for the acyclic phosphate clusters (Figure 1) are not the classic all *trans* conformations commonly encountered in the modeling of organic alkane chains. The minimized, low-energy structures show considerable curvature, with a large variation in the P-O-P and O-P-O bond angles due to the anisotropy of the P bonding, along with repulsive interactions. In general, the P-O-P bond angles range from 130° to 139°, while the terminal P-O-P bond angles in the smaller acyclic clusters were between 118° and 123°. These P-O-P bond angles compare to the 132° and 140° previously reported for the staggered and eclipsed conformations in the $H_4P_2O_7$ cluster, respectively [5]. The O-P-O bond angles range from 100° to 106°, with the O-P-O^T bond angles (T denotes the terminal P=O oxygen) ranging from 115° to 120°. The anisotropy of the O-P-O bond angles from the ideal tetrahedral angle of 109° is a major contributor to the non-linear minimized structures observed for the acyclic clusters (Figure 1). In the optimized acyclic clusters the observed P=O bond lengths are ~1.44 Å, the P-OH bond lengths range from ~1.54 to 1.57 Å, with the P-O-P bond lengths being ~1.61 Å. These bond lengths are slightly different than the previous *ab initio* results reported for the $H_4P_2O_7$ cluster [5], but these length differences result from the smaller basis set used for optimization in the present study: HF 6-31+G(d) versus B3LYP 6-311++G(2d,2p) in previous studies .

Because every phosphate tetrahedral contains a terminal P=O bond, the relative orientation of these terminal oxygen bonds can lead to different ring conformations. For example, in a cyclic phosphate cluster containing only two phosphorus atoms, the relative orientation of the terminal P=O bonds can be on the same side of the ring (*cis*) or on different sides of the ring (*trans*). These two different ring conformations will be designated as (+ +) and (+ −), respectively. This +/− notation will be used to designate the various ring conformations for the different sized cyclic phosphate clusters investigated, and are shown in Figures 2 and 3.

The ^{31}P CSA tensors for the acyclic phosphate clusters as a function of the number of phosphate tetrahedral were calculated and are given in Table 1. The isotropic chemical shielding, the individual tensor elements in the principal axis system (PAS), the tensor anisotropy and the CSA asymmetry parameter (as defined by Equations 1-3) are given. In the acyclic clusters there are both endgroup phosphate species (which contain two P-OH, one P=O and one P-O-P oxygen species) and a middle phosphate species (which contain one P-OH, one P=O, and two P-O-P oxygen species). In the larger acyclic clusters there is approximately a +10 ppm increase in the isotropic chemical shielding due to the change from a endgroup phosphate species to a middle phosphate species. The magnitude of this shift is similar to that observed experimentally between Q^3 and Q^2 or Q^2 and Q^1 phosphate species. A +18.8 ppm increase in shielding was noted between the endgroups and the middle phosphate species in a recent *ab initio* calculation of the ^{31}P CSA tensor in the $P_3O_{10}^{5-}$ cluster [7]. Experimentally an increase in shielding of +8.6 ppm and +10.8 ppm between the endgroup and middle phosphate species has been noted for the (**I**) and (**II**) crystal forms of the anhydrous $Na_5P_3O_{10}$ salts, respectively [14]. Similarly, in crystalline $K_5P_3O_{10}$ an increase of +15.0 to +18.3 ppm has also been reported [15, 16]. These experimental variations in the ^{31}P chemical shielding are of similar magnitude observed for the *ab initio* results on optimized acyclic clusters presented in Table 1. On the other hand, it should be remembered that these clusters represent truncated Q^3 species. In general, endgroup phosphates containing both terminal oxygen and two hydroxyl species are not commonly observed. Close inspection of these optimized structures suggest that simple variations in the P-O-P bond angle are responsible for the observed difference between endgroup and middle phosphate species. The $H_4P_2O_7$ cluster, which contains two endgroup species with a P-O-P bond angle of 135°, has an isotropic chemical shielding that is larger than observed for endgroup phosphate species in other clusters, and is within the same range seen for middle phosphate species (Table 1). Similarly, the $H_5P_3O_{10}$ cluster exhibits a smaller difference in the chemical shift between the endgroup and middle phosphate species, but contains P-O-P bond angles of 138° and 125°. For the larger acyclic clusters these terminal P-O-P bond angles are significantly smaller, ranging from 118° to 124°. Variation of the isotropic chemical shielding (σ_{iso}) as a function of the P-O-P bond angle and the torsional or dihedral angle between O_b-P-O_b and P-O_t (where O_b and O_t designate the bonding and terminal oxygens respectively) have been studied using both empirical and *ab initio* techniques [2, 3]. Variations on the order of 15 to 25 ppm have been calculated for σ_{iso} in Q^3 species due to changes in the P-O-P bond angle. The variation of the ^{31}P isotropic chemical shielding, as a function of P-O-P bond angle in the $H_4P_2O_7$ cluster have also been reported by Alam [5]. In those *ab initio* investigations it was shown that changes in the P-O-P bond angle was the structural variant that produced the largest change in the ^{31}P CSA tensor. For that simple cluster, the isotropic chemical shielding increased with larger P-O-P bond angles, consistent with the trends observed in the present study. For the $H_4P_2O_7$ cluster, changes in the O_b-P-O_b / P-O_t torsional angle ϕ had minimal effect on the isotropic chemical shielding, but did produce significant changes in the CSA anisotropy (~30 ppm) for torsional angles greater than ~80° [5]. Therefore, for the phosphate clusters reported in this manuscript, the observed variations in the ^{31}P CSA tensor are probably the result of changes in both the P-O-P bond angle and the O_b-P-O_b / P-O_t torsional angle.

Table 1. *Ab Initio* NMR ^{31}P CSA Tensors for Geometry Optimized Acyclic Phosphate Clusters.

Cluster	ID[a]	Species	σ_{iso}(ppm)	σ_{33}(ppm)	σ_{22}(ppm)	σ_{11}(ppm)	$\Delta\sigma$(ppm)	η
$H_4P_2O_7$	1	Endgroup	374.5	541.7	297.8	284.0	250.8	0.08
	2		374.5	541.7	297.8	284.0	250.8	0.08
$H_5P_3O_{10}$	1	Endgroup	360.1	483.4	323.0	274.0	184.9	0.40
	3		363.9	517.5	304.0	270.2	230.4	0.22
	2	Middle	366.2	483.3	327.7	287.7	175.6	0.34
$H_6P_4O_{13}$	1	Endgroup	364.9	506.1	314.5	274.1	211.8	0.29
	4		365.1	510.0	312.0	273.0	217.3	0.27
	3	Middle	373.1	523.1	310.0	286.0	225.1	0.16
	2		374.7	530.5	312.2	281.5	233.6	0.20
$H_7P_5O_{16}$	1	Endgroup	361.8	482.5	324.9	278.0	181.0	0.39
	5		362.7	481.6	326.8	279.7	178.3	0.40
	2	Middle	368.4	486.8	326.5	291.9	177.6	0.29
	3		373.7	538.5	311.4	271.1	247.3	0.24
	4		376.1	534.0	316.0	278.4	236.7	0.24
$H_8P_6O_{19}$	1	Endgroup	366.6	492.1	321.8	285.9	188.2	0.29
	6		368.1	516.8	318.4	268.9	223.2	0.33
	5	Middle	376.7	548.3	304.8	277.2	257.3	0.16
	3		377.3	540.4	311.7	279.7	244.7	0.20
	2		378.8	501.1	336.6	298.6	183.5	0.31
	4		379.1	534.6	326.9	275.8	233.3	0.33

[a] The ID number corresponds to the numbering of the individual P atoms in Figure 1.

The *ab initio* NMR simulations of the ^{31}P CSA tensor for the 2-,3- and 4- P membered phosphate rings are given in Table 2. The simulated ^{31}P CSA tensors for the different 5-P membered and 6-P membered cyclic clusters are given in Tables 3 and 4, respectively. These simulations also show a wide distribution of both the chemical shift and the anisotropy as a function of the number of phosphate tetrahedra in the cluster. Even for the cyclic phosphate clusters with constant number of phosphate tetrahedra, there are differences in the ^{31}P CSA tensor produced by the different conformations being investigated. Again these variations probably result from the combined effect of both P-O-P bond angle and O_b-P-O_b / P-O_t torsional angle variations.

The effects of cyclization for the smaller clusters are similar to previous calculations in phosphate systems. There is a +4 to +20 ppm increase in the chemical shielding noted for the phosphates between the cyclic $H_3P_3O_9$ (both conformations) and the middle phosphate species in the $H_5P_3O_{10}$ cluster (Table 1 and 2). *Ab initio* calculations of the $P_3O_{10}^{5-}$ and the cyclic $P_3O_9^{3-}$ Na-P species predicted a similar +7.1 ppm increase in the ^{31}P chemical shielding [7]. The isotropic chemical shielding for the $H_2P_2O_6$ cluster (Table 2) is not distinctly different from the other cyclic phosphate

Table 2. *Ab Initio* NMR ^{31}P CSA Tensors for Cyclic 2-, 3- and 4-P Membered Phosphate Clusters.

Cluster	ID[a]	Conformation	σ_{iso}(ppm)	σ_{33}(ppm)	σ_{22}(ppm)	σ_{11}(ppm)	$\Delta\sigma$(ppm)	η
$H_2P_2O_6$	1	(+ +)	373.8	574.7	278.3	268.3	301.4	0.05
	2		381.2	599.9	281.7	262.1	328.0	0.09
	1	(− +)	379.1	591.4	284.0	261.9	318.5	0.10
	2		379.1	591.4	284.0	261.9	318.5	0.10
$H_3P_3O_9$	1	(+ + +)	386.9	583.4	293.0	284.3	294.8	0.04
	2		386.9	583.4	293.0	284.3	294.8	0.04
	3		387.0	583.6	293.0	284.4	294.9	0.04
	3	(+ + −)	370.4	511.2	316.1	284.0	211.2	0.22
	1		387.5	587.2	293.7	281.4	299.7	0.06
	2		387.5	587.2	293.7	281.4	299.7	0.06
$H_4P_4O_{12}$	1	(+ + + +)	381.8	544.6	307.1	293.6	244.3	0.08
	2		381.8	544.6	307.1	293.6	244.3	0.08
	3		384.8	555.5	302.7	296.3	256.0	0.04
	4		384.8	555.5	302.7	296.3	256.0	0.04
	3	(+ + + −)	379.0	532.7	311.9	292.5	230.5	0.13
	1		379.8	522.5	326.3	290.4	214.2	0.25
	2		383.3	555.5	298.3	296.2	258.3	0.01
	4		386.2	580.8	298.5	279.4	291.9	0.10
	1	(+ + − −)	391.6	563.1	312.0	299.7	257.3	0.07
	2		391.6	563.1	312.0	299.7	257.3	0.07
	3		391.6	563.1	312.0	299.7	257.3	0.07
	4		391.6	563.1	312.0	299.7	257.3	0.07
	1	(+ −+ −)	375.8	512.1	320.7	294.6	204.4	0.19
	2		375.9	517.4	317.8	292.4	212.3	0.18
	3		386.7	578.4	300.9	280.9	287.5	0.10
	4		390.0	584.6	304.8	280.7	291.9	0.12

[a] The ID number corresponds to the numbering of the individual P atoms in Figure 2.

clusters reported in this study. In contrast the shielding anisotropy ($\Delta\sigma$) is nearly 50 to 100 ppm larger than any of the other phosphate clusters reported. This large tensor anisotropy results from the very strained ring structure, where the P-O-P bond angle (within the ring plane) is only 94° and 95° for the *cis* and *trans* configuration, respectively. The internal O-P-O bond angles are also highly distorted, being approximately 85°. For the $H_3P_3O_9$ clusters (Figure 2) the structural distortions are less severe, but the P-O-P bond angles still range between 121° and 139°; smaller than the average P-O-P bond angle observed in the acyclic and larger cyclic phosphate clusters. For the $H_4P_4O_{12}$, $H_5P_5O_{15}$ and $H_6P_6O_{18}$ clusters (Figures 2 and 3) the P-O-P bond angles range from 129° to 150°. For these larger cyclic phosphate clusters the observed range of isotropic chemical shielding is very broad ranging from +370

Table 3. *Ab Initio* NMR CSA Tensors for Cyclic 5-P Membered Phosphate Clusters.

Cluster	ID[a]	Conformation	σ_{iso}(ppm)	σ_{33}(ppm)	σ_{22}(ppm)	σ_{11}(ppm)	$\Delta\sigma$(ppm)	η
$H_5P_5O_{15}$	5	(+ + + + +)	382.0	543.1	310.8	292.0	241.7	0.12
	3		382.2	552.4	304.1	290.2	255.2	0.08
	2		383.3	548.3	308.4	293.4	247.4	0.09
	1		384.3	556.2	299.5	297.2	257.8	0.01
	4		385.4	560.0	302.5	293.8	261.8	0.05
	3	(+ + + + −)	375.9	515.8	320.1	291.8	209.9	0.20
	5		381.4	561.6	303.3	279.4	270.3	0.13
	1		383.7	554.9	299.8	296.3	256.9	0.02
	2		384.3	546.7	312.3	294.0	243.6	0.11
	4		388.6	564.7	302.6	298.4	264.3	0.02
	3	(+ + + − −)	376.1	519.8	317.9	290.7	215.5	0.19
	5		381.1	561.7	303.2	278.3	270.9	0.14
	1		383.8	551.2	305.5	294.9	251.0	0.06
	2		385.1	546.9	311.7	296.6	242.8	0.09
	4		387.7	563.9	301.2	298.1	264.3	0.02
	3	(+ + − + −)	375.2	515.5	318.8	291.2	210.5	0.20
	1		377.9	518.7	323.4	291.7	211.2	0.23
	2		379.8	532.8	320.8	285.7	229.6	0.23
	5		381.6	563.8	301.7	279.5	273.2	0.12
	4		388.7	585.3	302.7	278.1	294.9	0.13

[a] The ID number corresponds to the numbering of the individual P atoms in Figure 3.

ppm to nearly +395 ppm (Table 2-4). There does not appear to be any simple correlation between cluster ring size and tensor values (except for the highly strained $H_2P_2O_6$ cluster). Correlations between the isotropic shielding, the shielding anisotropy and the cluster size are discussed later in this section.

The absolute isotropic chemical shielding values (σ_{iso}) presented in Tables 1-4 can be converted to chemical shifts (δ) relative to 85% H_3PO_4 by comparison to the chemical shielding of PH_3 at the same level of theory using [11]

$$\delta(\text{calc}) = \sigma(PH_3, \text{calc}) - \sigma_{iso}(\text{calc}) - 266.1 \text{ppm}. \tag{5}$$

This relationship is based on the experimental chemical shift of PH_3 ($\delta = 266.1$ ppm). The shielding for PH_3 at this level of theory has already been reported as 590.1 ppm [5].

The asymmetry of the CSA tensor (η) is also variable (see Tables 1-4), ranging from 0.01 (a symmetric environment) to 0.40. The smaller or highly symmetric clusters commonly show symmetric ^{31}P CSA tensors. For example, the (+ + + +), and the (+ + − −) conformations in the $H_4P_4O_{12}$ clusters are predicted to have very small η values. In general, there does not appear to be any

Table 4. *Ab Initio* NMR CSA Tensors for Cyclic 6-P Membered Phosphate Clusters.

Cluster	ID[a]	Conformation	σ_{iso}(ppm)	σ_{33}(ppm)	σ_{22}(ppm)	σ_{11}(ppm)	$\Delta\sigma$(ppm)	η
$H_6P_6O_{18}$	5	(+ + + + + +)	378.4	543.1	305.6	286.4	247.1	0.12
	6		384.0	546.4	313.9	291.7	243.6	0.14
	1		385.5	564.6	307.8	284.1	268.6	0.13
	4		387.7	567.0	306.7	289.3	269.0	0.10
	2		389.8	579.1	303.3	287.1	284.0	0.09
	3		390.6	578.8	308.0	285.1	282.3	0.12
	6	(+ + + + + −)	377.4	487.8	334.7	309.7	165.6	0.25
	5		379.3	534.8	313.0	289.9	233.3	0.15
	1		383.7	566.5	302.4	282.4	274.1	0.11
	2		387.8	574.9	307.2	281.3	280.6	0.14
	3		388.5	576.9	303.1	285.4	282.7	0.09
	4		388.9	567.0	308.4	291.3	267.1	0.10
	5	(+ + + − − −)	380.1	492.5	341.6	306.2	168.5	0.31
	1		383.2	565.3	303.9	280.3	273.3	0.13
	6		383.9	509.7	336.1	305.9	188.7	0.24
	3		385.4	561.8	307.7	286.8	264.6	0.12
	2		387.5	577.2	305.9	279.5	284.5	0.14
	4		394.9	587.4	308.8	288.5	288.8	0.11
	6	(+ + + + − −)	378.0	488.5	341.2	304.3	165.8	0.33
	5		382.0	508.5	332.4	305.2	189.7	0.22
	1		382.3	564.0	303.1	279.9	272.5	0.13
	3		386.7	561.7	311.2	287.1	262.6	0.14
	2		390.0	579.9	306.7	283.5	284.8	0.12
	4		390.1	581.5	309.5	279.2	287.1	0.16
	3	(+ − + − − −)	371.5	507.0	322.5	284.9	203.3	0.28
	6		374.3	477.4	332.3	313.4	154.5	0.18
	5		379.9	546.8	304.7	288.3	250.3	0.10
	2		381.3	553.7	314.0	276.2	258.6	0.22
	1		384.7	565.6	305.5	283.0	271.3	0.12
	4		388.8	586.7	298.0	281.7	296.8	0.08
	3	(+ − + − + −)	370.2	503.7	322.6	284.3	200.3	0.29
	6		375.2	481.6	331.3	312.7	159.6	0.17
	2		380.3	549.5	315.7	275.7	253.8	0.24
	5		380.6	550.5	305.5	285.7	254.9	0.12
	1		383.7	565.1	302.7	283.4	272.1	0.11
	4		388.2	585.5	298.0	281.2	295.9	0.09

[a] The ID number corresponds to the numbering of the individual P atoms in Figure 3.

absolute correlation between η and the size of the cluster, or whether the cluster was cyclic or acyclic. For the cyclic phosphate clusters it was noted that the phosphate species with larger η typically had smaller $\Delta\sigma$, but this trend is not universal, and does not extend to the acyclic phosphate clusters investigated (see Tables 2-4).

Figure 4 shows the correlation between the ^{31}P isotropic chemical shielding (σ_{iso}) and the CSA anisotropy ($\Delta\sigma$) as a function of the number of phosphates in the both acyclic and cyclic clusters. There are regions were distinct differences between the ^{31}P CSA tensors for cyclic and acyclic clusters are observed: most notably for the 2-P, 3-P and 4-P-membered phosphate rings. The dotted lines in Figure 4 are for visual separation of these regions. For cyclic clusters $\Delta\sigma$ is typically greater than $\sim$ +250 ppm, with σ_{iso} being larger than $\sim$ +375 ppm. The acyclic clusters tend to have smaller tensor values than cyclics, with values of +250 ppm and +375 ppm for $\Delta\sigma$ and σ_{iso}, respectively. This distinction between cyclic and acyclic phosphate clusters disappears for the 5-P and 6-P-membered rings, where overlap between the predicted cyclic and acyclic ^{31}P CSA parameters was observed. This loss of distinct differences in the larger cyclic clusters was expected since these are 10- and 12-membered rings (P and O) where the possible ring conformations do not require as many restrictive structural constraints. It is interesting to note that the highly strained 2-P-membered ring conformations [8] have a larger anisotropy ($\sim$ +325 ppm) than any of the other cyclic clusters, as was discussed earlier in this section.
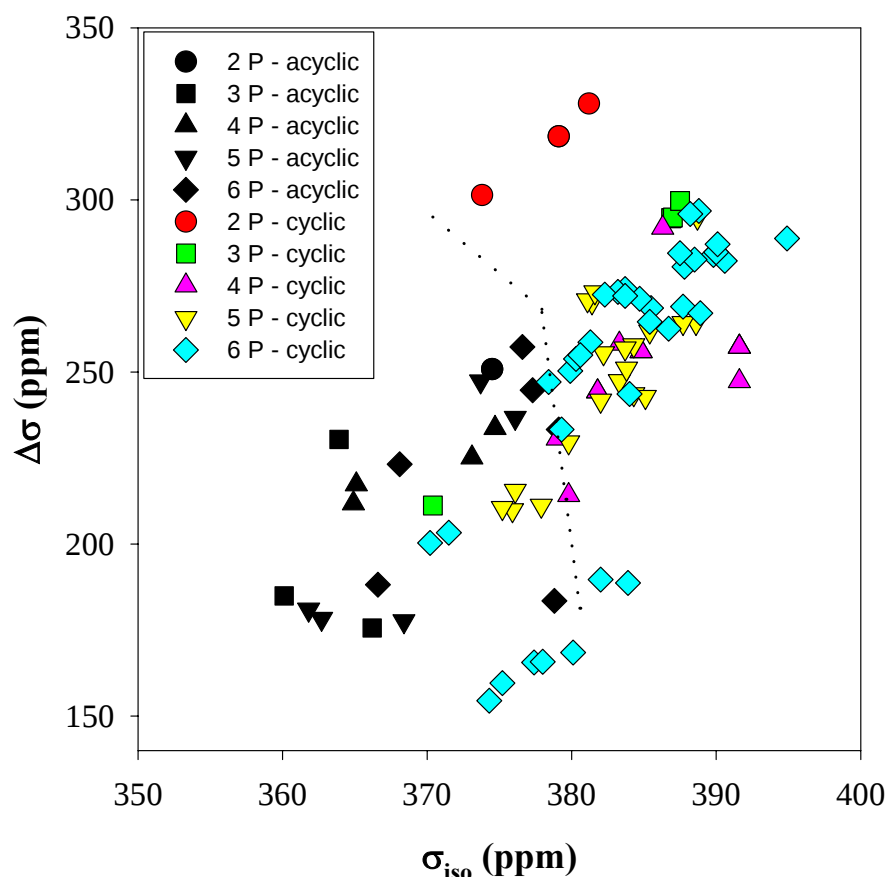

Figure 4. The calculated ^{31}P CSA isotropic chemical shielding (σ_{iso}) versus shielding anisotropy ($\Delta\sigma$) for different sized acyclic and cyclic phosphate clusters.

Effect of Cyclization on Orientation of CSA Tensor

In general the chemical shielding tensor contains both symmetric and antisymmetric components. The antisymmetric components of the shielding tensor, as well as other non-secular components, contribute only in second order to the observed frequency, and can be readily neglected [17]. The GAUSSIAN 98 output contains both the symmetric and antisymmetric tensor components. To determine the relative orientation of the CSA tensor, it is therefore necessary to decompose the ^{31}P CSA tensor ($\boldsymbol{\sigma}$) into the symmetric ($\boldsymbol{\sigma}_{sy}$), and antisymmetric ($\boldsymbol{\sigma}_{asy}$) components [18]

$$\boldsymbol{\sigma} = \boldsymbol{\sigma}_{sy} + \boldsymbol{\sigma}_{asy} \tag{6}$$

The antisymmetric components of $\boldsymbol{\sigma}$ are given by

$$\boldsymbol{\sigma}_{asy} = \frac{1}{2}\left(\boldsymbol{\sigma} - \boldsymbol{\sigma}^{\mathrm{T}}\right) \tag{7}$$

where $\boldsymbol{\sigma}^{\mathrm{T}}$ is the transpose. The symmetric component $\boldsymbol{\sigma}_{sy}$ is therefore the only part of concern, and is diagonal in the PAS, with the eigenvalues of this diagonal representation being used in description of the ^{31}P CSA tensor through Equations 1- 4.

The relative orientation of the CSA tensor in the PAS and the tensor orientation in the molecular coordinate system allows additional changes in the tensor due to cyclization to be addressed. The representation of the CSA tensor (symmetric portion only) in the PAS is diagonal and will be denoted by $\boldsymbol{\sigma}^{\mathrm{D}}$. The matrix representation of the CSA tensor in a different coordinate system ($\boldsymbol{\sigma}$), in this case the molecular frame representation given by GAUSSIAN 98, can be realized by a transformation between the two coordinate systems according to [18]

$$\boldsymbol{\sigma}^{\mathrm{D}} = \mathbf{R}_{\mathrm{D}}^{-1}\boldsymbol{\sigma}\mathbf{R}_{\mathrm{D}} \tag{8}$$

where $\mathbf{R}_{\mathrm{D}}$ is the rotation matrix. This can be reduced to a principal-value relationship

$$\mathbf{R}_{\mathrm{D}}\boldsymbol{\sigma}^{\mathrm{D}} = \boldsymbol{\sigma}\mathbf{R}_{\mathrm{D}} \Leftrightarrow \vec{\mathbf{r}}_n\sigma_n = \boldsymbol{\sigma}\vec{\mathbf{r}}_n \tag{9}$$

where σ_n are the eigenvalues of the matrix $\boldsymbol{\sigma}$, and the eigenvectors $\vec{\mathbf{r}}_n$ are the column vectors of the rotation matrix $\mathbf{R}_{\mathrm{D}}$. These eigenvectors describe the orientation of the PAS in the molecular coordinate axis system. A more detailed description of these transformations is given in Reference [18].

Figure 5 shows the relative orientation of the ^{31}P CSA tensor in the acyclic 5-P-member cluster. Only the central portion of the acyclic phosphate cluster is shown for clarity. The largest principal component σ_{33} is oriented approximately 173° from the terminal P=O bond axis (nearly collinear).
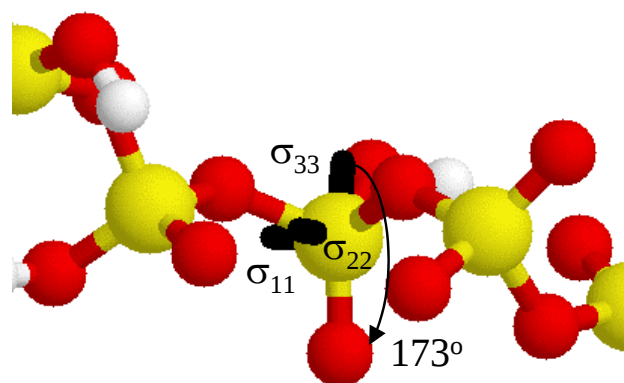
Figure 5. Relative orientation of the ^{31}P CSA tensor for the central phosphate in the acyclic 5-P-membered cluster. The σ_{33} principal component lies ~ 173° from the terminal P=O bond. Some intervening hydrogen atoms have been removed for clarity.

Both the σ_{11} and σ_{22} tensor elements split the P-O-P bond projection, and are not collinear with either the P-OH or the P-O-P bonds. In general, due to the lack of bonding symmetry only the σ_{33} element is approximately collinear with any of the P-O bonds in these clusters.

The relative orientation of the ^{31}P CSA tensor for the 2-P-membered *cis* (+ +) and *trans* (+ −) cyclic cluster is shown in Figure 6. For both the *cis* and *trans* cluster the σ_{33} principal component is nearly parallel to the terminal P=O bond vector (~12°-13°), while the projection of the σ_{22} component bisects the two P-O-P bonds forming the ring, and the σ_{11} component lies in the plane of the 2-P-membered ring. The orientation of the σ_{22} tensor element between the two bridging oxygen atoms forming the ring is consistent with the high anisotropy observed for these smaller cyclic clusters (see Table 2 and Figure 2). The largest principal component σ_{33} is still approximately along the terminal P=O bond.

Figure 7 shows the orientation of the ^{31}P CSA tensor for a single phosphate tetrahedral (σ_{iso} = 383.3 ppm, ID #2, see Table 3) in the (+ + + + +) 5-P-membered cyclic cluster. There are slightly different orientations of the CSA tensor depending on which specific phosphate is being investigated, but this single example is illustrative of the tensor orientations observed in the larger cyclic clusters. The σ_{33} principal component is approximately 174° from the terminal P=O direction (or about 6° from the P=O axis), with the σ_{11} and σ_{22} tensor elements not being collinear with either the P-OH or the P-O-P bonds. These results are similar to the results seen in the larger acyclic clusters (See Figure 5), as well as the 2-P membered cyclic clusters (Figure 6). For the 2-P membered cyclics the small asymmetry parameter means that σ_{11} and σ_{22} are very similar, but are defined through Equation 4. Reversal of the σ_{11} and σ_{22} principal components would result in the σ_{33} tensor element being pointed in the same general direction as the σ_{33} tensor elements in Figures 5 and 7.
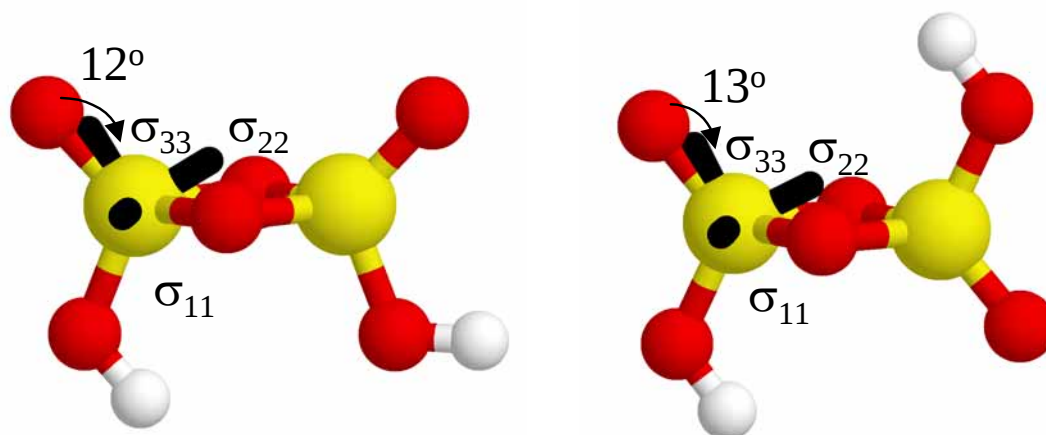
Figure 6. The relative orientation of the ^{31}P CSA tensor in the *cis* (+ +) and the *trans* (+ −) configurations in the 2-P-membered cyclic phosphate clusters. The orientation of the tensor is nearly identical in both configurations, with the σ_{33} principal axis being ∼12° from the terminal P=O bond.
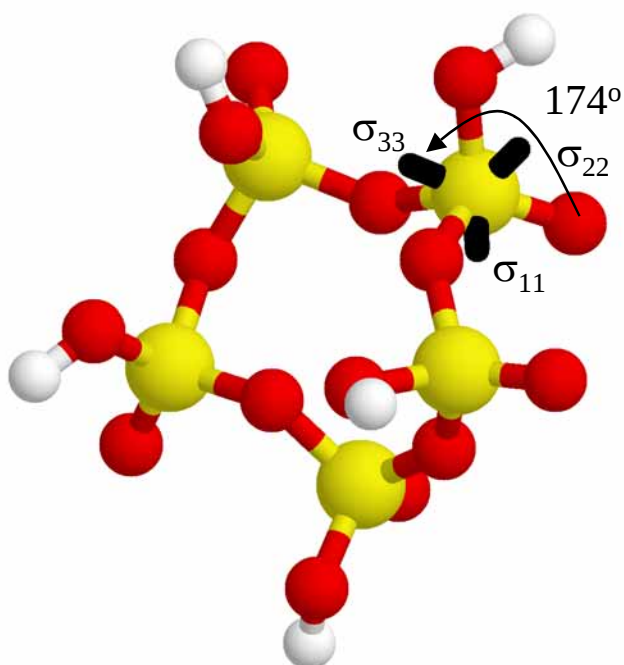
Figure 7. The relative orientation of the ^{31}P CSA tensor (only one specific phosphate shown for clarity) in the (+ + + + +) 5-P-membered cyclic cluster. The σ_{33} principal component lies ∼ 174° from the direction of the terminal P=O bond.

.

Discussion

The ^{31}P NMR CSA tensors for a series of acyclic and cyclic phosphate clusters has been analyzed using *ab initio* GIAO calculations. As seen in Figure 4, there are distinct differences in both the isotropic shielding (σ_{iso}) and tensor anisotropy ($\Delta\sigma$) noted for acyclic and cyclic phosphate clusters, most notably for the smaller 2-P, 3-P and 4-P-membered cyclic systems. For the larger 5-P and 6-P-membered cyclic clusters these differences diminish as a result of the reduced conformational constraints.

So the original question still remains. Are any of the ^{31}P CSA tensor parameters distinct enough to be used as an indicator of cyclic versus acyclic systems in amorphous phosphate systems? Based on the *ab initio* cluster calculations reported here, the answer is yes for certain type of cyclic systems. For the smaller 2-P, 3-P and 4-P-membered ring clusters (known to have higher internal ring strain energy), both $\Delta\sigma$ and σ_{iso} are significantly larger than that observed in simple linear or acyclic phosphate clusters. Therefore if it was someway possible to isolate different species based on this increase in the chemical shift and/or anisotropy, the formation of rings versus chains in complex systems could be determined from NMR observables.

Experimentally this proposition may prove to be very difficult, especially in cases where changes in the modifier concentration or the production of hydrated species can produce similar changes in the chemcial shielding. For example, in the ^{31}P MAS NMR investigations of lithium ultraphosphate glasses by Alam and Brow [19], the anisotropy ($\Delta\sigma$) for the Q^3 phosphate species ranged from 200 to 255 ppm. A crude argument based on Figure 4 would suggest that these phosphate species are predominantly linear in nature, without a high concentration of rings. This conclusion is in contrast to arguments based on MD simulations [8]. The effect of Li modifier concentration, and/or Li position, on the resulting shielding anisotropy has yet to be explored. In the investigations of Losso and co-workers [3], they found that the position of the modifier produced significant variations on the isotropic chemical shielding. Therefore in complex systems there may be many factors contributing to the variations in the chemical shielding that should be considered in making such arguments. In very controlled systems, where there is a predominance of a given structure, and other variations such as modifier concentration or hydroxyl formation does not occur, the identification of cyclic versus acyclic phosphate clusters becomes more realistic.

References

1. In *Modeling NMR Chemical Shifts, Gaining Insights into Structure and Environment*, Facelli, J. C. and de Dios, A. C. Eds., American Chemical Society: Washington, DC, 1999.
2. Sternberg, U., Pietrowski, F. and Priess, W. The Influence of Structure and Coordination on the ^{31}P-Chemical Shift in Phosphates. *Zeitschrift Physik. Chemie neue Folge* **1990**, *168*, 115-128.

3. Losso, P., Schnabel, B., Jager, C., Sternberg, U., Stachel, D. and Smith, D. O. ^{31}P NMR Investigations of Binary Alkaline Earth Phosphate Glasses of Ultraphosphate Composition. *J. Non-Cryst. Solids* **1992**, *143*, 265-273.

4. Alam, T. M., Ab Initio Calculation of Nuclear Magnetic Resonance Chemical Shift Anisotropy Tensors I. Influence of Basis Set on the Calculation of [31]P Chemical Shifts, Sand98-2053, Sandia National Laboratories, 1998.

5. Alam, T. M., "*Ab Initio Calculations of ^{31}P NMR Chemical Shielding Anisotropy Tensors in Phosphates: The Effect of Geometry on Shielding*" In *Modeling NMR Chemical Shifts, Gaining Insights into Structure and Environments,* J. C. Facelli and A. C. de Dios Ed., American Chemical Society: Washington, DC, 1999.

6. Márquez, A., Sanz, J. F. and Odriozola, J. A. Theoretical Investigation of NMR Chemical Shieldings on the AlPON Catalyst System. *J. Non-Cryst. Solids* **2000**, *263-264*, 189-194.

7. Cody, G. D., Mysen, B., Sághi-Szabó, G. and Tossell, J. A. Silcate-Phosphate Interaction in Silicate Glasses and Melts: I. A Multinuclear (^{27}Al, ^{29}Si, ^{31}P) MAS NMR and *Ab Initio* Chemical Shielding (^{31}P) Study of Phosphorous Speciation in Silicate Glasses. *Geochimica et Cosmochimica Acta* **2001**, *65*, 2395-2411.

8. Liang, J.-J., Cygan, R. T. and Alam, T. M. Molecular Dynamics Simulation of the Structure and Properties of Lithium Phosphate Glasses. *J. Non-Cryst. Solids* **2000**, *263&264*, 167-179.

9. Gaussian 98, A.6: Frisch, M. J., Trucks, G. W., Schlegel, H. B., Scuseria, G. E., Robb, M. A., Cheeseman, J. R., Zakrezewski, V. G., Montgomery, J. A., Stratmann, R. E., Burant, J. C., Dapprich, S., Millam, J. M., Daniels, A. D., Kudin, K. N., Strain, M. C., Farkas, O., Tomasi, J., Barone, V., Cossi, M., Cammi, R., Mennucci, B., Pomelli, C., Adamo, C., Clifford, S., Ochterski, J., Petersson, G. A., Ayala, P. Y., Cui, Q., Morokuma, K., Malick, D. K., Rabuck, A. D., Raghavachari, K., Foresman, J. B., Cioslowski, J., Ortiz, J. V., Stefanov, B. B., Liu, G., Liashenko, A., Piskorz, P., Komaromi, I., Gomperts, R., Martin, R. L., Fox, D. J., Keith, T., Al-Laham, M. A., Peng, C. Y., Nanayakkara, A., Gonzalez, C., Challacombe, M., Gill, P. M. W., Johnson, B., Chen, W., Wong, M. W., Andres, J. L., Gonzalez, C., Head-Gordon, M., Replogle, E. S. and Pople, J. A.: Pittsburg, PA, 1998.

10. Ditchfield, R., Hehre, W. J. and Pople, J. A. Self-Consistent Molecular-Orbital Methods. IX. An Extended Gaussian-Type Basis for Molecular-Orbital Studies of Organic Molecules. *J. Chem. Phys.* **1972**, *54*, 724-728.

11. van Wüllen, C. A Comparison of Density Functional Methods for the Calculation of Phosphorus-31 NMR Chemical Shifts. *Phys. Chem. Chem. Phys* **2000**, *2*, 2137-2144.

12. Sebastiani, D. and Parrinello, M. A New *Ab-Initio* Approach for NMR Chemical Shifts in Periodic Systems. *J. Phys. Chem* **2001**, *105*, 1951-1958.

13. Tossell, J. A. and Sághi-Szabó, G. Aluminosilicate and Borosilicate Single 4-Rings: Effects of Counterions and Water on Structure, Stability and Spectra. *Geochimica et Cosmochimica Acta* **1997**, *61*, 1171-1179.

14. Griffiths, L., Root, A., Harris, R. K., Packer, K. J., Chippendale, A. M. and Tromas, F. R. Magic-angle Spinning Phosphorus-31 Nuclear Magnetic Resonance of Polycrystalline Sodium

Phosphates. *J. Chem. Soc. Dalton Trans.* **1986**, 2247-2251.

15. Grimmer, A. R. and Haubenreisser, U. High-Field Static and MAS ^{31}P NMR: Chemical Shift Tensors of Polycrystalline Potassium Phosphates P_2O_5 $x$$K_2O$ (0<x<3). *Chem. Phys. Lett.* **1983**, *99*, 487-490.

16. Duncan, T. M. and Douglass, D. C. On the [31]P Chemical Shift Anisotropy in Condensed Phosphates. *Chem. Phys.* **1984**, *87*, 339-349.

17. Mehring, M. *Principles of High Resolution NMR in Solids*; Springer-Verlag, Berlin, 1983; 1-342.

18. Schmidt-Rohr, K. and Spiess, H. W. *Multidimensional Solid-State NMR and Polymers*; Academic Press, San Diego, 1994; 1-478.

19. Alam, T. M. and Brow, R. K. Local Structure and Connectivity in Lithium Ultraphosphate Glasses: A Solid-State ^{31}P MAS NMR and 2D Exchange Investigation. *J. Non-Cryst. Solids* **1998**, *223*, 1-20.